THE JOURNAL OF COMPARATIVE NEUROLOGY 245:301-318 (1986)

Optic Tectum of the Eastern Garter Snake, *Thamnophis sirtalis*. IV. Morphology of Afferents From the Retina

DENNIS M. DACEY AND PHILIP S. ULINSKI
Department of Anatomy and Committee on Neurobiology, The University of Chicago, Chicago, Illinois 60637

ABSTRACT

The morphology of single retinal terminals in the optic tectum of the eastern garter snake was demonstrated by orthograde filling from extracellular injections of horseradish peroxidase (HRP) into the optic tract. HRP-filled terminals share a characteristic shape and structure. Their parent axons course caudally in the stratum opticum within fascicles of 200–300 fibers of varying diameters. Single axons exit a fascicle and course into either the stratum fibrosum et griseum superficiale, ventrally, or the stratum zonale, dorsally, where they bifurcate successively two or three times into preterminal branches. Each preterminal branch gives rise to many thin, terminal branchlets laden with boutons. The arbors are ellipsoidal with their long axes oriented mediolaterally and their short axes oriented rostrocaudally. Arbors vary in their overall size (from 45 to 150 μm), in the diameters of their parent axons (from less than 0.5 to 3.0 μm), and in the size of their terminal boutons (from 0.5 to 3.5 μm). Bouton size increased with increasing diameter of the parent axon. The great majority of arbors are confined to one of three retinorecipient sublayers in the superficial tectum. However, the full range of arbor sizes and axon diameters is present in each sublayer.

Key words: retinotectal terminals, horseradish peroxidase, axon morphology

This is the fourth in a series of papers that describes the organization of the optic tectum at the light microscopic level in the eastern garter snake, *Thamnophis sirtalis*. The previous papers described the morphology of the dendrites and axons of efferent and intrinsic tectal neurons that were filled with horseradish peroxidase (HRP) (Dacey and Ulinski, '86a,b,c). This paper begins a study of tectal afferents by describing the morphology of retinal axons in the tectum. Small extracellular, iontophoretic injections of horseradish peroxidase into the optic tract were used to demonstrate single retinotectal terminals. The results suggest that the great majority of retinal arbors share a characteristic shape and branching pattern and are restricted to one of three retinorecipient sublayers in the tectum. There is a significant variation among the arbors in axon diameter, terminal bouton size, and in overall arbor size, but there is no apparent relation between laminar position and the morphology of a given arbor. These findings are used to assess the relationships between retinal arbors and morphologically identified tectal neurons that have been described in the previous papers in this series.

MATERIALS AND METHODS

Four techniques were used to study the retinotectal projection in *Thamnophis*. First, the retinotectal projection was demonstrated autoradiographically in ten snakes. Equal parts of ^{3}H-leucine and proline (1 μCi/μl) were reconstituted in 0.9% saline to a final concentration of 10 μCi/μl. Five microliters of the solution were slowly infused into the vitreal chamber of one eye in each animal over a 30-minute period. The animals were perfused with a phosphate-buffered 4% paraformaldehyde solution after 3–10 days survival. Brains were embedded in paraffin and sectioned at 15 μm. Mounted sections were coated with Kodak NTB-2 emulsion, exposed for 4 weeks, and developed in Kodak D-19 for 6 minutes.

Second, the detailed morphology of retinotectal arbors was examined by using the orthograde transport of HRP.

Accepted September 25, 1985.

Methods for HRP injections and reaction protocol and for morphological analysis have been described in detail in the previous three papers (Dacey and Ulinski, '86a,b,c). The present results are derived from animals that received iontophoretic injections of HRP at various points along the optic tract from the optic chiasm to the pretectum. Twenty-five cases were available for study.

Third, axon morphology in the superficial layers of the tectum was also examined in Golgi preparations of 100 brains impregnated by variants of the Kopsch (Colonnier, '64) and classical rapid methods (Valverde, '70) Brains were embedded in celloidin and sectioned at 80–150 μm in the coronal or horizontal planes.

Finally, the fascicles of axons that run rostrocaudally through the stratum opticum were examined with electron microscopic techniques. Snakes were anesthetized with Nembutal and then perfused intracardially with about 100 ml of 0.15 M phosphate buffer, pH 7.3, followed by 200 ml of a solution of 4% paraformaldehyde, 5% glutaraldehyde, and 4% sucrose in phosphate buffer. The brains were removed 2 hours after perfusion, immersed another 2 hours in the fixative, and cut into transverse slices about 1 mm thick. These were immersed for 2 hours in 2% osmic acid, dehydrated, stained in 2% uranyl acetate, and embedded flat in the caps of inverted BEEM capsules. The block face was trimmed to include the full depth of the optic tectum. Thin sections with silver or gray interference colors were cut with a diamond knife and mounted on bar grids. Photographs of axon fascicles were taken at 3,800× and enlarged to an overall magnification of 8,428×. The long axes of axon profiles cut in cross section were measured to the nearest 0.1 μm.

RESULTS

The retinal terminal zone

In order to determine how the morphology and spatial distribution of single HRP-filled retinotectal arbors is related to the overall retinal terminal field the total projection was first demonstrated by autoradiographic tracing. The results generally confirm a previous silver degeneration study in *Thamnophis* (Halpern and Frumin '73). The silver grain distribution resulting from a tritiated leucine and proline injection into one eye shows that the retinotectal projection is completely crossed (Fig. 1). Label is present in the stratum zonale, the interfascicular spaces of the stratum opticum, and sublayers a, b, and c of the stratum fibrosum et griseum superficiale. Grain density was not uniform across these layers, being high in the cell-poor sublayers a and c, and low in sublayer b, a narrow layer of cell bodies. Labeling in the stratum zonale was also heavy, but was isolated from labeling in the stratum fibrosum et griseum superficiale by the axon fascicles in the stratum opticum. These fascicles were not labeled and appear as oval, grain-free patches. Labeling above the background level ends sharply at the border between the stratum fibrosum et griseum superficiale and stratum griseum centrale.

This silver grain pattern suggests that the retinal projections in *Thamnophis* terminate in three distinct sublayers in the superficial tectum. The following results describe the morphology of individual HRP-filled retinal terminals and consider the spatial relation of these terminals to the three-tiered pattern of the overall projection.

IDENTIFICATION OF RETINOTECTAL TERMINAL ARBORS

Most of the terminal arbors presented in this study were anterogradely filled from HRP injections made at various points along the optic tract in the diencephalon. Although the great majority of axons in the optic tract are undoubtedly of retinal origin, it is possible that some fraction are non-retinal, arising from injections which impinged upon pathways to the tectum from diencephalic structures. Thus some of the HRP-filled arbors may not originate from retinal ganglion cells. However, several observations indicate that the axons travel in the stratum opticum and there is no evidence for nonretinal afferents in this fiber layer (Dacey and Ulinski, '86d). Second, the laminar position of the arbors is consistent with the results of autoradiographic tracing of the total retinotectal projection, as outlined in the previous section of the Results. Third, the morphology of the arbors is distinct from the morphology of non-retinal afferents that also project to the retinorecipient sublayers (Dacey and Ulinski, '86d).

Morphology of individual terminal arbors

Most of the retinal terminals in Golgi and HRP preparations shared a characteristic structure and shape. A terminal arbor stained by the Golgi method illustrates this pattern (Fig. 2). The entire terminal is restricted to a single sublayer—sublayer a of the stratum fibrosum et griseum superficiale in this example. The parent axon arises from the lower border of the stratum opticum and descends to the center of the sublayer where it splits successively into several thinner preterminal branches. Each preterminal branch radiates from the central branch point of the primary axon. The preterminal branches issue thin, terminal branchlets laden with boutons. The boutons tend to appear singly along the terminal branchlets, separated from other boutons by several microns. Small clusters of boutons occasionally appear at the ends of a terminal branchlet or when two or more branchlets appose or intertwine. The terminal branchlets follow a meandering course and often branch or recurve within the arbor.

Variation in this basic branching pattern occurs in two ways. First, one or all of the preterminal branches may extend for some distance without branching before giving rise to terminal branchlets. In this situation the preterminal branches originate from the parent axon outside the field of terminal boutons (e.g., Fig. 5, the arbor on the right). Second, terminal branchlets may arise from the parent axon before it gives rise to preterminal branches (e.g., Fig. 5, the arbor on the left). Despite this variation in branching pattern, the overall shape of the arbor, as defined by the spatial distribution of the terminal boutons, is not altered.

Single arbors are ellipsoidal with their long axes oriented mediolaterally and short axes rostrocaudally. For example, the arbor shown in Figure 2 measures 100 μm along its mediolateral axis and 65 μm along its rostrocaudal axis. The great majority of arbors are restricted to a single sublayer of the retinal terminal zone, as defined in the autoradiographic preparations, but extend across the full thickness of their sublayer (e.g., Fig. 2). The thickness of an arbor (its

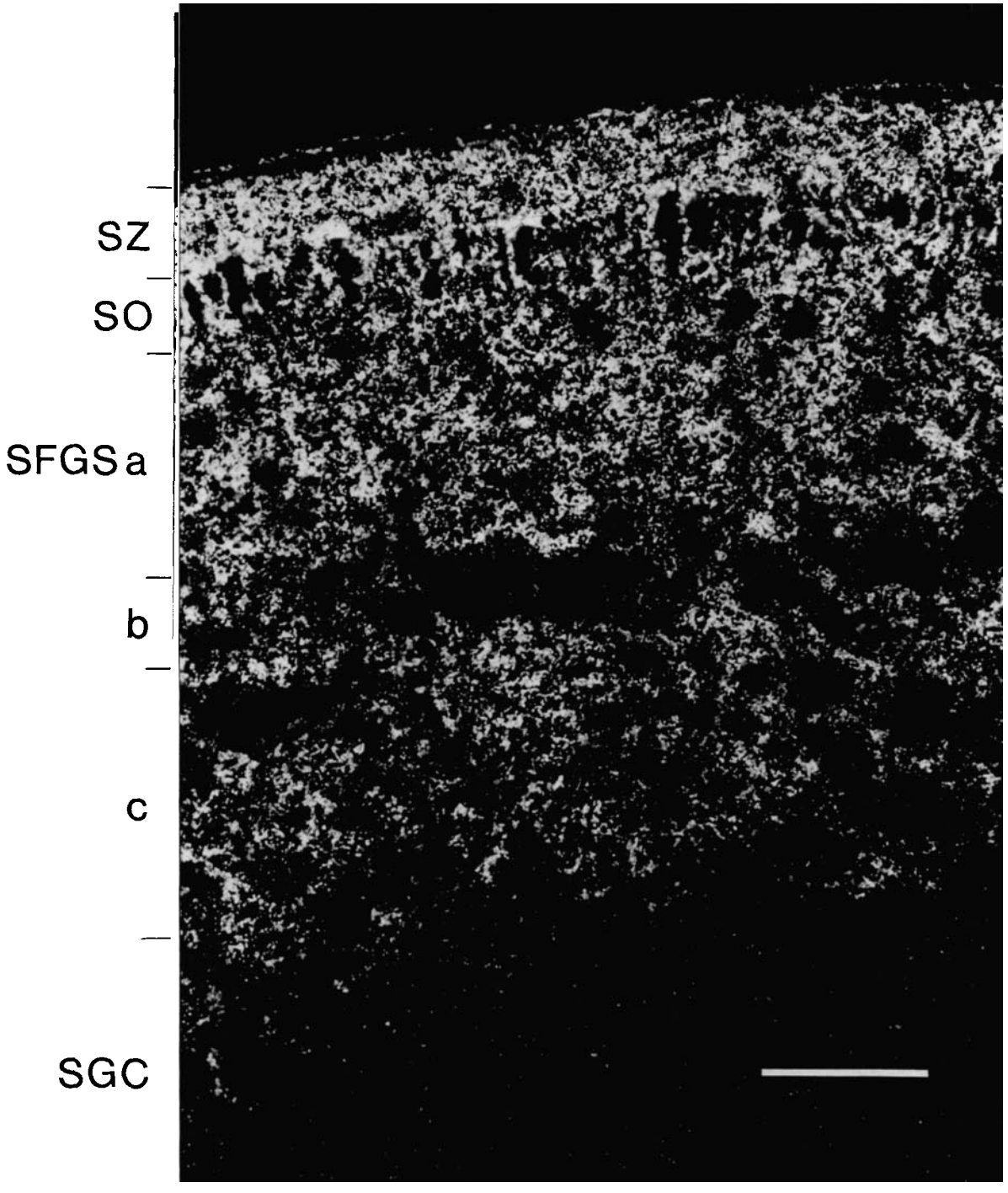

Fig. 1. Autoradiographic labeling of the retinorecipient tectal layers after intraocular injection of tritiated amino acids. This darkfield photomicrograph shows heavy labeling over the stratum zonale (SZ) and sublayers a and c of the stratum fibrosum et griseum superficiale (SFGS). Labeling above background ceases abruptly at the border between sublayer c and the stratum griseum centrale (SGC). Scale bar = 50 μm.

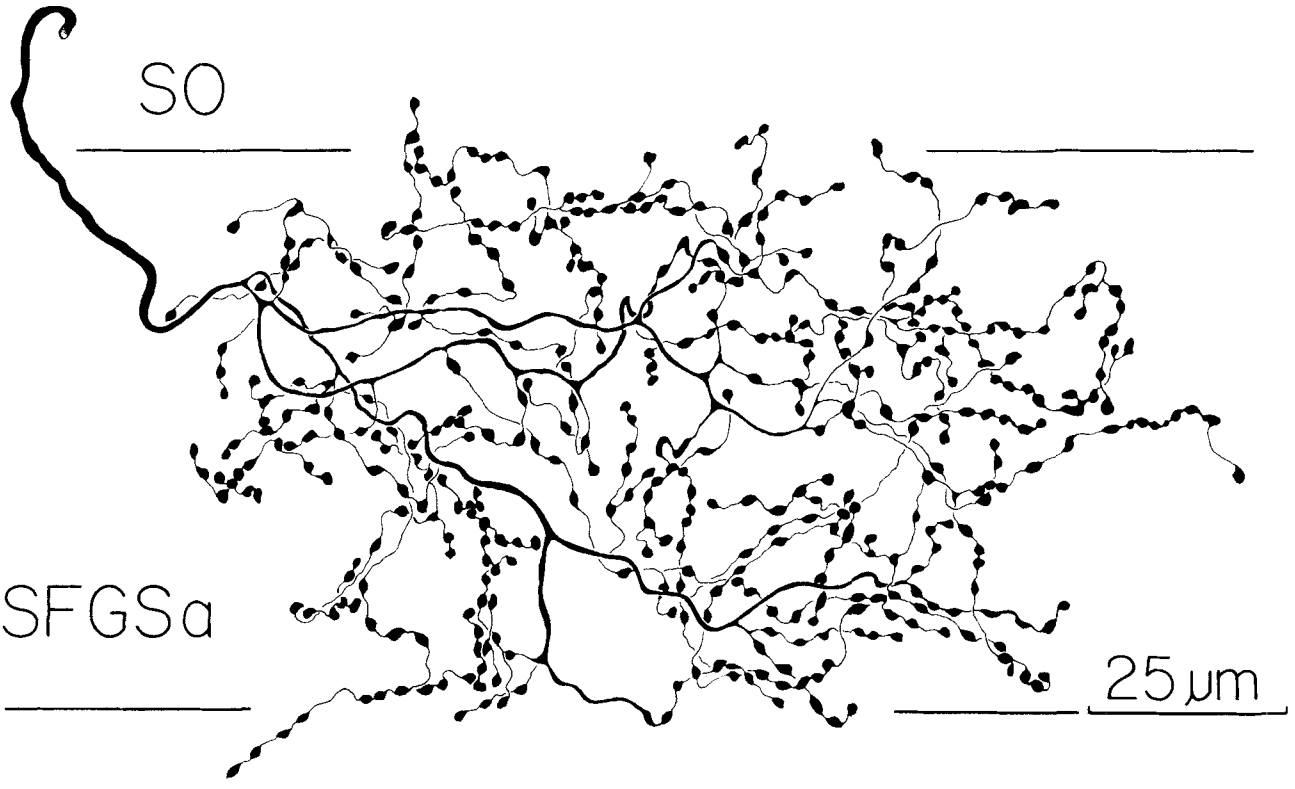

Fig. 2. Camera lucida tracing of rapid Golgi impregnation of an axon terminal restricted to sublayer a of the stratum fibrosum et griseum superficiale. The primary axon descends from the stratum opticum, splitting into several preterminal branches that give rise to thin, terminal branchlets laden with boutons. The overall shape of the arbor is ellipsoidal with its long axis oriented mediolaterally.

dorsoventral axis) is therefore determined by its laminar position. Arbors in the stratum zonale are 25–35 μm thick whereas those in sublayer a or c of the stratum fibrosum et griseum superficiale are 60–65 μm thick. With few exceptions (Fig. 13), the three retinorecipient sublayers reflect a laminar segregation of single terminal arbors.

Variation in the morphology among terminal arbors

Eighty-six HRP-filled arbors were sampled from much of the rostrocaudal extent of the tectum and from each retinorecipient sublayer. Although all the arbors share a characteristic shape and structure, there is significant variation in the overall sizes of the arbors, the diameters of their primary axons in the tectum, and in the average size of the terminal boutons on a given arbor. Table 1 presents a summary of the morphological variation in the HRP-filled arbors. To illustrate this variation, detailed camera lucida tracings of 19 HRP-filled arbors are shown in Figures 5–13.

The diameters of the primary axons of these arbors range from 0.5μm to 3.0 μm (Table 1, Fig. 4). To determine how this relatively small sample relates to the total population of retinotectal axons, the diameters of axons in several fascicles within the stratum opticum were measured in electron micrographs. A total of 1,662 axons from 12 fascicles distributed across the tectum were measured. The results are shown in Figure 3 and are similar to those obtained by Reperant et al. ('81) in the asp viper. The histogram shows that the great majority of axons are relatively thin, between 0.5 and 1.0 μm in diameter. Comparison of the histograms from the HRP and electron microscopic samples show that the HRP-filled axons encompass the full size range of parent axons but that the larger axons, from 1.0 to 3.0 μm in diameter, are overrepresented in the sample. A probable explanation for this is that the larger-diameter axons are more easily and completely filled from an extracellular injection of HRP.

TABLE 1. Summary of the Morphological Variation in 86 HRP-Filled Retinotectal Arbors

No. of axons	Axon diameter (μm)[1]	Bouton size (μm)[2]	Arbor size (μm)[3]
19	2.5–3.0	1.0–3.5	50–150
8	2.0–2.5	1.0–3.5	60–130
9	1.5–2.0	0.5–2.0	50–150
21	1.0–1.5	0.5–2.0	45–150
9	0.5–1.0	0.5–1.0[4]	50–130
20	≤0.5	0.5–1.0	50–140

[1]All measurements were taken with the aid of an eyepiece graticule. One division on the graticule equaled 0.5 μm at a total magnification of ×1,560.
[2]The majority of boutons are fusiform structures; the measurements shown are of their long axes.
[3]Arbors are ellipsoidal in shape; the measurements shown are of their long axes.
[4]Two axons in this range had large boutons, 2.0–3.0 μm, and are illustrated in Figure 8.

The terminal boutons on single HRP-filled arbors are relatively uniform in size. However, they tend to increase

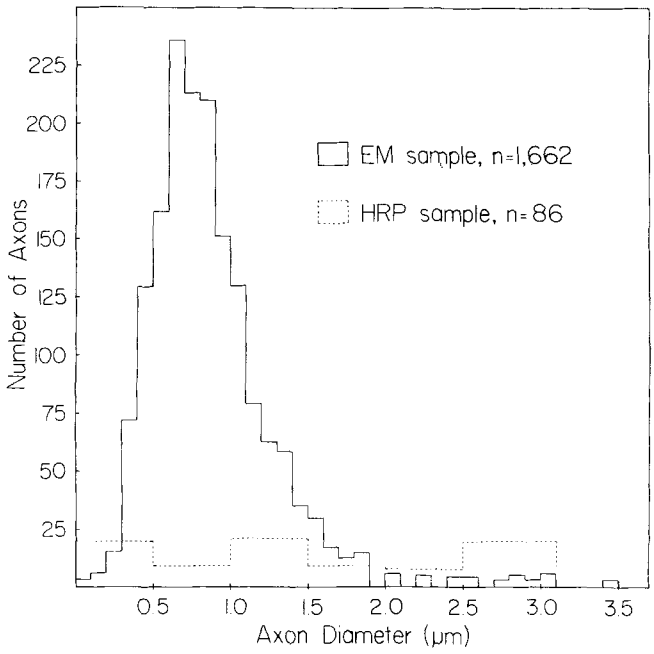

Fig. 3. Diameters of retinotectal axons. The histogram outlined with the dotted line shows the diameters of the parent axons of HRP-filled retinotectal arbors. These axons were measured to the nearest 0.5 μm with the light microscope at a total magnification of ×1,560. The histogram outlined with the solid line shows the diameters of axons sampled in the stratum opticum and measured to the nearest 0.1 μm from electron micrographs at a total magnification of ×8,428. Comparison of the two histograms suggests that the HRP-filled sample includes nearly the full range of axon diameters, as assessed with the greater resolution of the electron microscope, but that the larger caliber axons, from 1.0 to 3.0 μm, are overrepresented in the HRP sample.

in size with increasing diameter of the parent axon (Table 1, Fig. 4). Figure 5 shows two arbors that span sublayer c of the stratum fibrosum et griseum superficiale. They have large-caliber axons, about 2.5 μm in diameter, and bear large terminal boutons that range in size from 2.0 to 3.5 μm along their long axes. By contrast, the two arbors shown in Figure 6 have axon diameters of about 1.5 μm and boutons that range from 0.5 to 2.0 μm in size. Figure 7 illustrates two arbors with still smaller parent axons of less than 0.5 μm in diameter and small boutons that range in size from 0.5 to 1.0 μm along their long axes. The correspondence between axon diameter and bouton size held for 84 of the 86 arbors in the sample. The two exceptions have thin axons, 0.5–1.0 μm, but a majority of large boutons from 2.0 to 3.0 μm in diameter (Fig. 8).

The retinotectal arbors also varied in overall size, ranging from 45–150 μm along their long axes (Figs. 8, 9, 10). The majority of arbors in the sample (70 of 86) were of similar size, measuring 90–100 μm in the mediolateral axis and 60–65 μm in the rostrocaudal axis. There was no clear relation between axon diameter (or bouton size) and the size of the arbors. Figure 9 illustrates three arbors with thin axons, 0.5–1.0 μm in diameter, whose arbors range from 45 to 110 μm along their long axes. The largest arbor with a thin axon measured about 130 μm along its long axis (Fig. 7, top). Similarly, Figure 10 illustrates two arbors located in sublayer c with axon diameters of 2.5–3.0 μm and large boutons, but different overall sizes. The arbor on the left measures about 150 μm along the long axis and the arbor on the right measures about 100 μm.

The variation in the axon diameters and sizes of the arbors was not related to the laminar location of the arbors. Thus, the full range of parent axon size was observed in each of the three retinorecipient sublayers. Arbors with large diameter axons (2.0–3.0 μm) restricted to the stratum zonale and sublayer a are illustrated in Figure 11 and are comparable to arbors of similar dimensions but located in sublayer c (Figs. 5, 10). Similarly, arbors with thinner axon diameters, 0.5–2.0 μm, showed no laminar preference (Figs. 6, 7, 9, 12).

Eight axons (9%) in the sample had terminal arbors that were not restricted to one of the three terminal sublayers defined by autoradiography but extended across two adjacent sublayers. All eight of these bilayered arbors showed terminal branchlets that passed from sublayer a into the overlaying stratum zonale via the interfascicular zones of the stratum opticum (Fig. 13). These arbors ranged in axon diameter from 1.0 to 2.5 μm. The distribution of boutons across the stratum zonale and sublayer a was uneven in four of the bilayered arbors; only a few terminal branchlets extend up through the stratum opticum (Fig. 13, left). In each of the others, the parent axon gives rise to terminal branchlets in sublayer a before ascending to the stratum zonale where it arborizes profusely to produce a second distribution of boutons that extends from the pial surface through the stratum opticum (Fig. 13, right).

DISCUSSION

Variations in the morphology of retinotectal terminal arbors

Previous observations of retinal terminal arbors in Golgi preparations of the tectum of both mammals and nonmammals suggest that retinal arbors vary considerably in shape and structure (e.g., Ramón y Cajal, '11; Lazar and Szekely, '67). For example, it has been suggested that in both pigeons and lizards some optic axons may collateralize and give rise to multiple terminal arbors (Stone and Freeman, '71; Quiroga, '78). Arbors with several different branching patterns were recognized in a Golgi study of the bullfrog tectum (Potter, '72). The results of Golgi studies must be interpreted with caution, however, because of the difficulty in acquiring arbors that appear impregnated to their finest branches and because of the probability that some of the arbors may originate from nonretinal sources. By contrast, recent intracellular and extracellular HRP studies of the morphology of retinotectal arbors in frogs (Lazar, '84; Stirling and Merrill, '85), teleost fish (Ito et al., '84), hamsters (Sachs and Schneider, '84), and the present results in the garter snake all provide more detailed descriptions of the structure of the arbors. These descriptions emphasize variations in laminar position, axon diameter, and overall arbor size rather than variations in shape and structure. In hamsters, arbors have been classified into two broad groups by differences in axon diameter, bouton size, and laminar position (Sachs and Schneider '84). In *Thamnophis*, arbors could not be simply classified on the basis of morphological

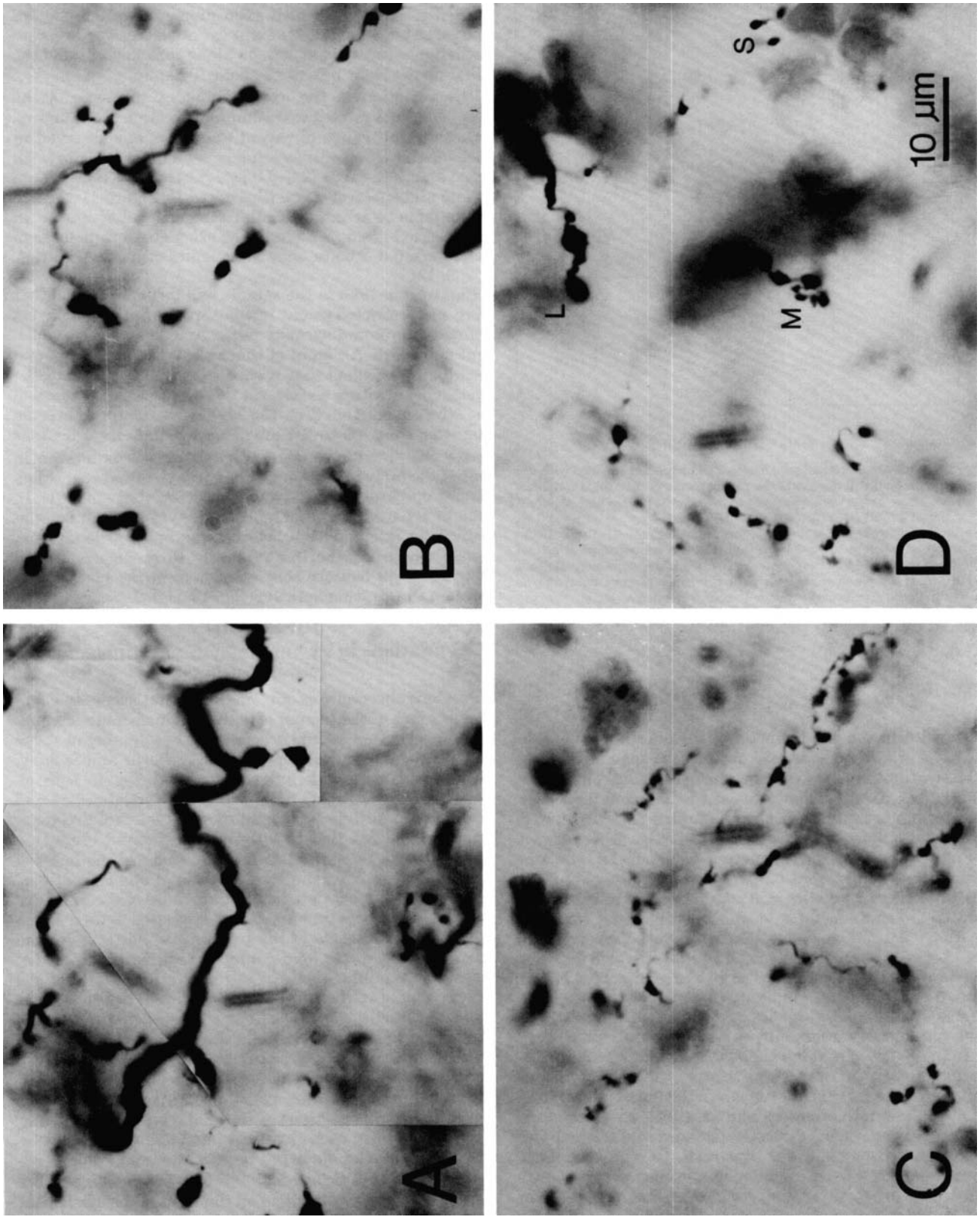

Fig. 4. Photomicrographs of retinotectal terminal arbors. This figure illustrates the range in terminal bouton size observed on HRP-filled arbors. The smallest boutons are shown in A and progressively larger boutons are shown in B and C. D. Boutons from arbors with large (L), 2.0–2.5 μm, medium (M), 1.0–1.5 μm, and small (S), 0.5 μm or less, parent axon diameters.

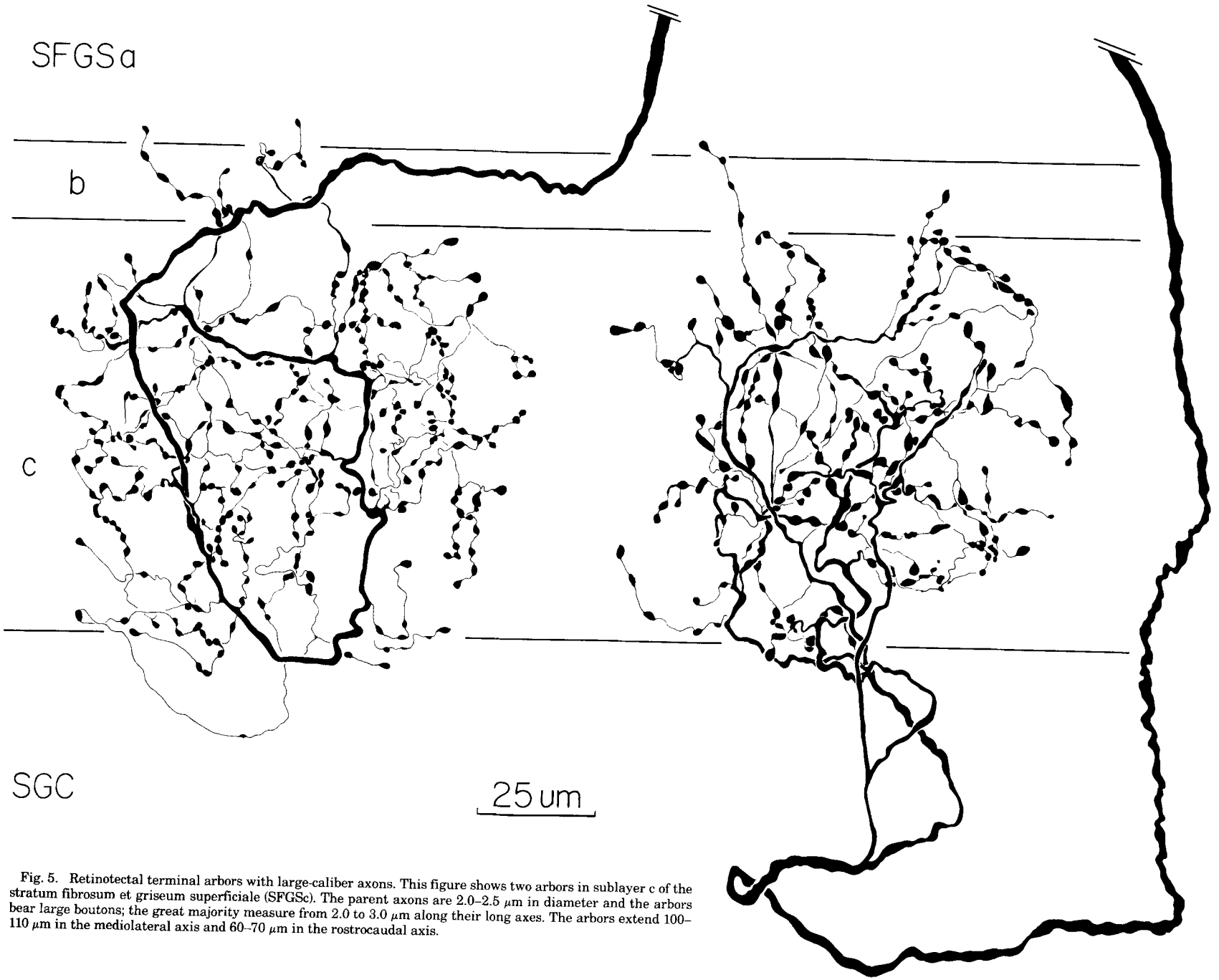

Fig. 5. Retinotectal terminal arbors with large-caliber axons. This figure shows two arbors in sublayer c of the stratum fibrosum et griseum superficiale (SFGSc). The parent axons are 2.0–2.5 μm in diameter and the arbors bear large boutons; the great majority measure from 2.0 to 3.0 μm along their long axes. The arbors extend 100–110 μm in the mediolateral axis and 60–70 μm in the rostrocaudal axis.

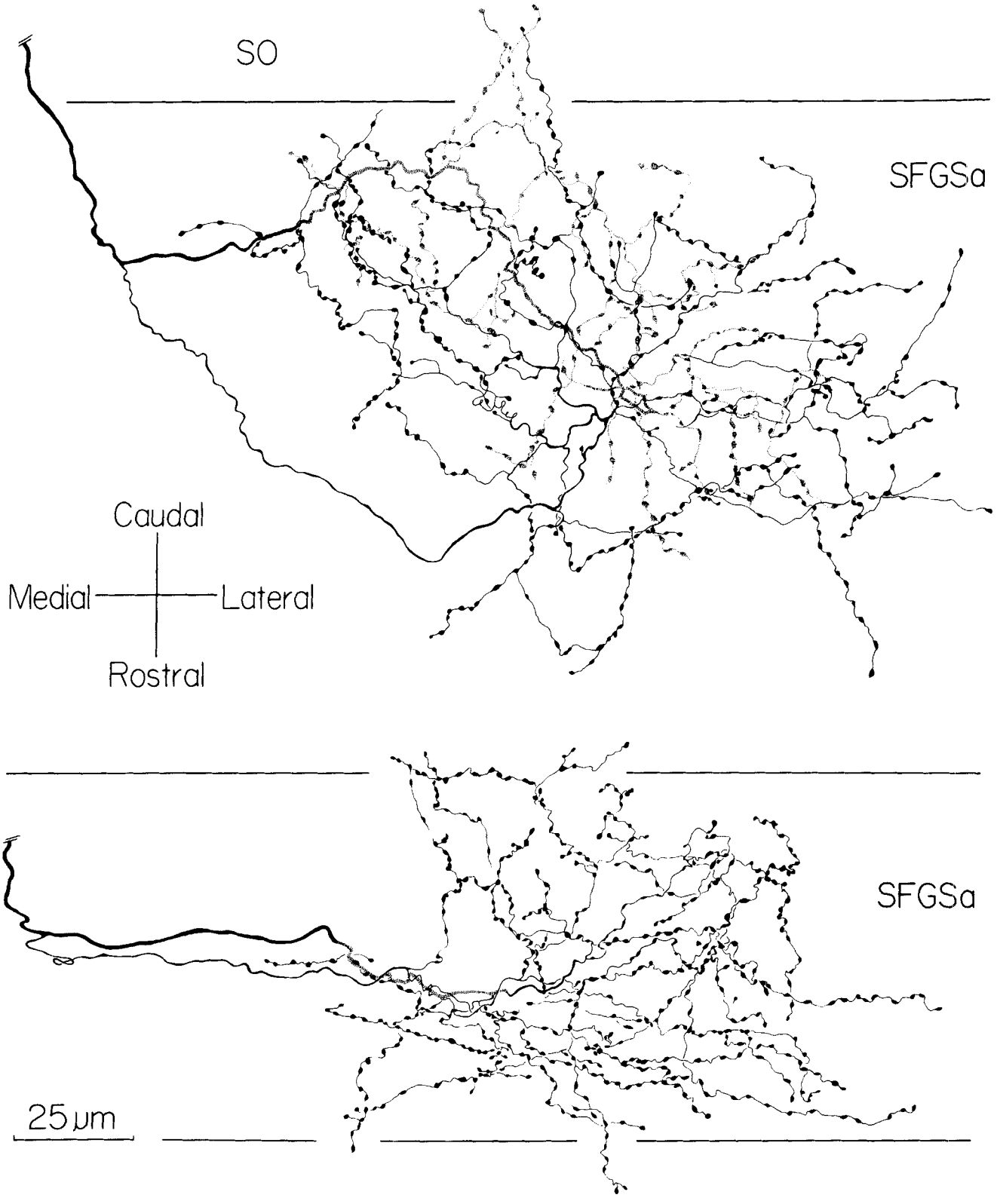

Fig. 6. Retinotectal terminal arbors with medium-caliber axons. Two arbors with axon diameters of 1.0–1.5 μm are shown in sublayer a of the stratum fibrosum et griseum superficiale. These arbors bear boutons that are relatively uniform in size; the great majority measure between 1.0 and 1.5 μm along their long axes. The upper arbor is taken from horizontal sections through sublayer a; it extends 80–100 μm, rostrocaudally and 125–150 μm mediolaterally.

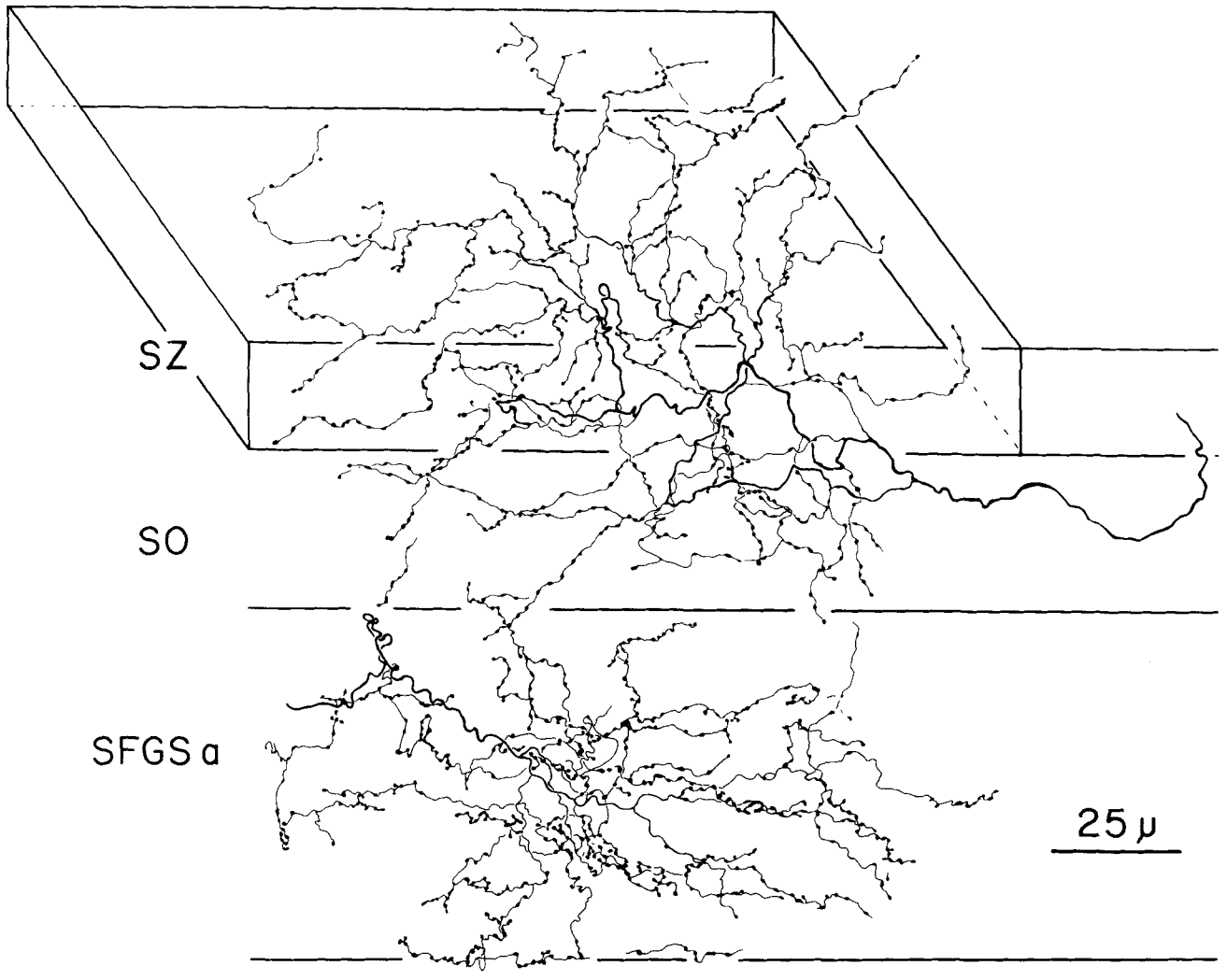

Fig. 7. Retinotectal terminal arbors with small-caliber axons. Arbors with axon diameters of 0.5 μm or less are shown in the stratum zonale and sublayer a of the stratum fibrosum et griseum superficiale. They bear small boutons that range in size from 0.5 to 1.0 μm along their long axes. The upper arbor was traced in a plane that passed obliquely through the stratum zonale; the box that surrounds the arbor thus illustrates its rostrocaudal extent. Arbors measure 115–130 μm in their mediolateral axes and 70–80 μm in the rostrocaudal axes.

features because the great majority were ellipsoidal, with their long axes oriented mediolaterally, and showed a characteristic preterminal and terminal branching pattern. However, the arbors varied in axon diameter, terminal bouton size, and overall size.

The variation in axon diameter is probably correlated with variation in the overall morphology of retinal ganglion cells projecting to the tectum. Retinal wholemounts in *Thamnophis* reveal a range of ganglion cell soma sizes (unpublished observations). Nothing is known of the dendritic morphology or physiological properties of these ganglion cells, but Golgi studies in lizards (Ramón y Cajal, '33) and turtles (Kolb, '82) show that, as in other vertebrate groups, retinal ganglion cells in reptiles display a variety of morphologies. Moreover, there are correlations between dendritic morphology, soma size, axon diameter, conduction velocity, and response to light in turtle ganglion cells (Marchiafava and Weiler, '80; Marchiafava and Wagner, '81; Peterson and Ulinski, '82; Geri et al., '82), comparable to those seen in other vertebrate groups (reviews: Rodieck, '79; Grusser-Cornehls, '84; Vanegas et al., '84). If there is a similar relationship between ganglion cell soma size and axon diameter in *Thamnophis*, then the largest-caliber axons would originate from ganglion cells with the largest somata and thinner axons from cells with progressively smaller somata. Further, given the large number of morphological types of ganglion cells that are currently being identified in both mammals (Kolb et al.,'81; Dacey, '84; Leventhal et al., '85) and nonmammals (Kolb '82), small differences in the branching patterns, axon diameters, and arbor sizes may be related to specific ganglion cell types (e.g., Stirling and Merrill, '85).

In *Thamnophis* there is a clear correspondence between axon caliber and terminal bouton size, such that boutons

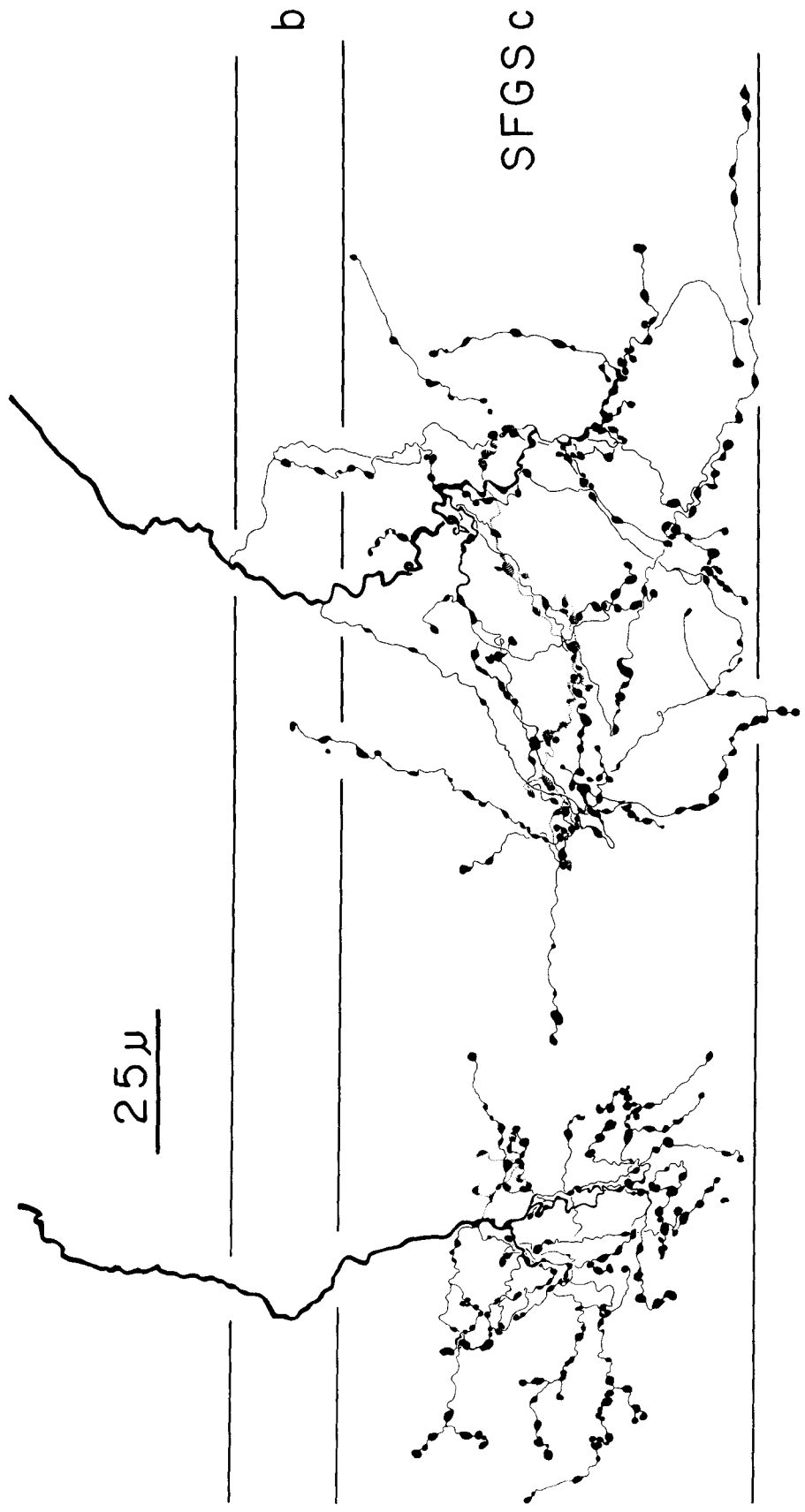

Fig. 8. This figure shows two arbors with medium caliber parent axons about 1.0 μm in diameter but many large boutons, 2.0–2.5 μm along their long axes. The arbor on the left was one of the smallest in the sample (about 55 μm along its long axis) whereas the arbor on the right measures 110–125 μm along its long axis.

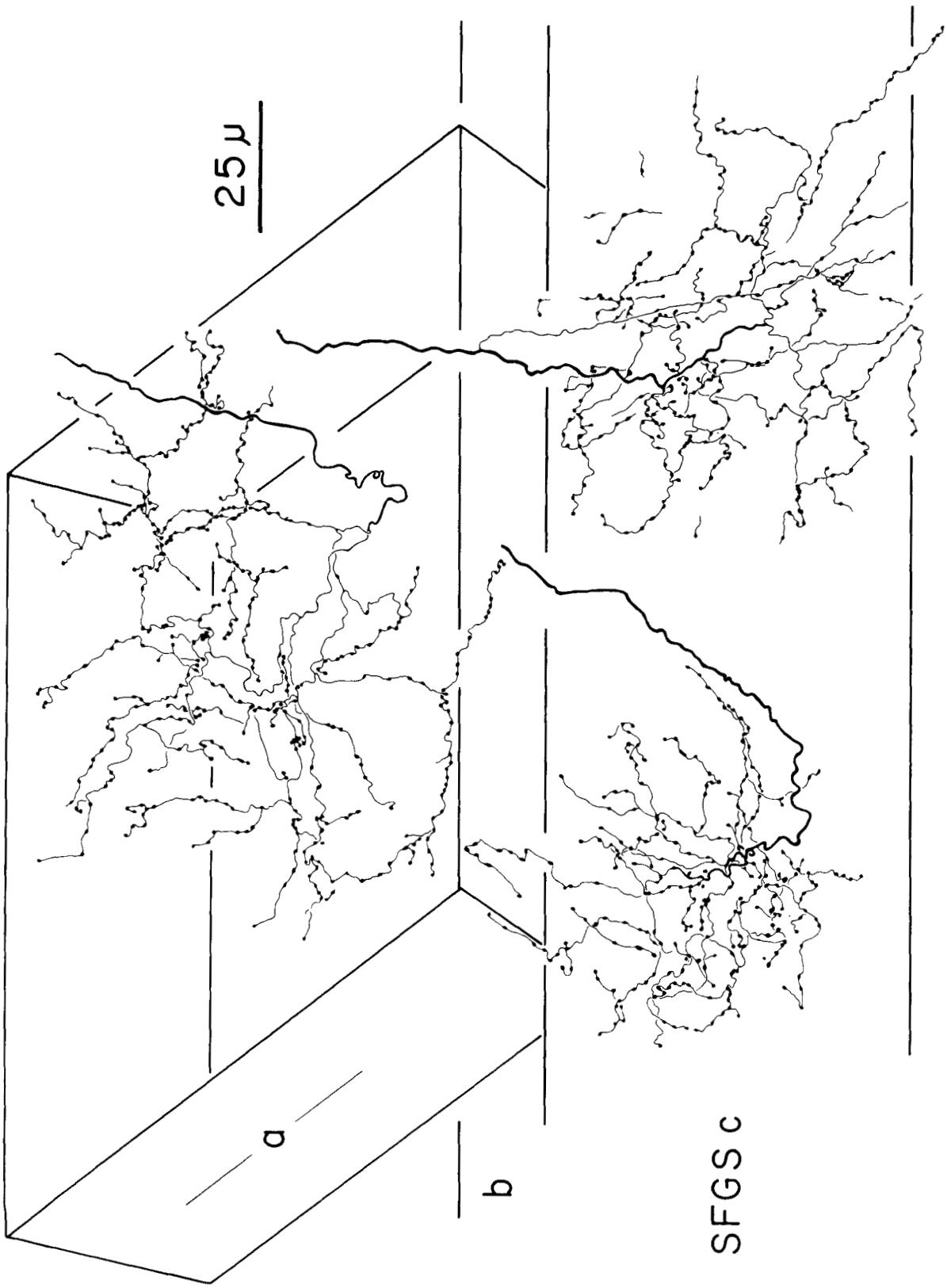

Fig. 9. Size variation in arbors with small-caliber axons. These three arbors have parent axons of 0.5 μm or less in diameter. Arbors with thin axons vary in overall size from 130 μm (see Fig. 7) to 50 μm along their long axes. The arbors shown in this figure range in size from 50 μm (lower left) to 110 μm (upper arbor).

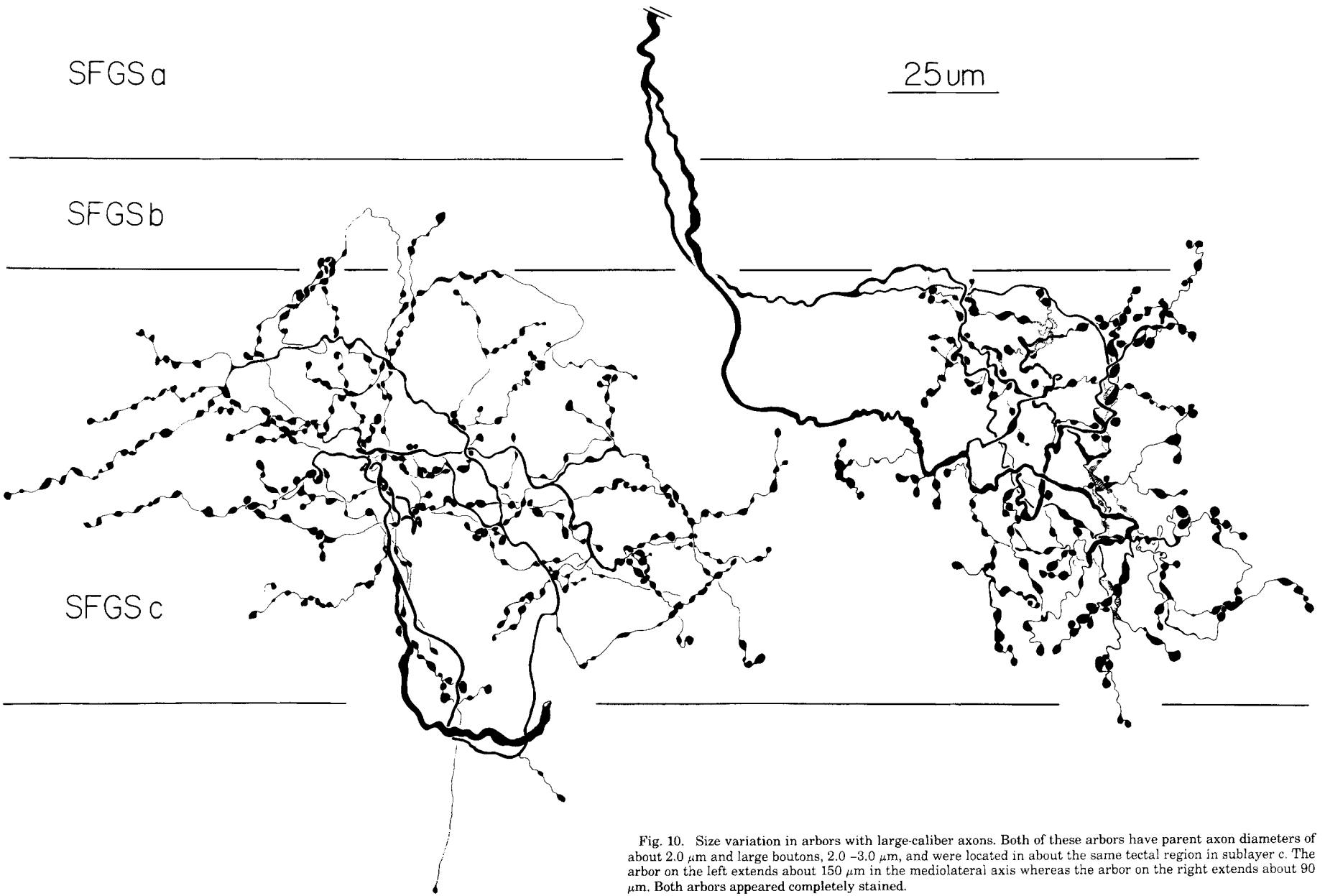

Fig. 10. Size variation in arbors with large-caliber axons. Both of these arbors have parent axon diameters of about 2.0 μm and large boutons, 2.0 –3.0 μm, and were located in about the same tectal region in sublayer c. The arbor on the left extends about 150 μm in the mediolateral axis whereas the arbor on the right extends about 90 μm. Both arbors appeared completely stained.

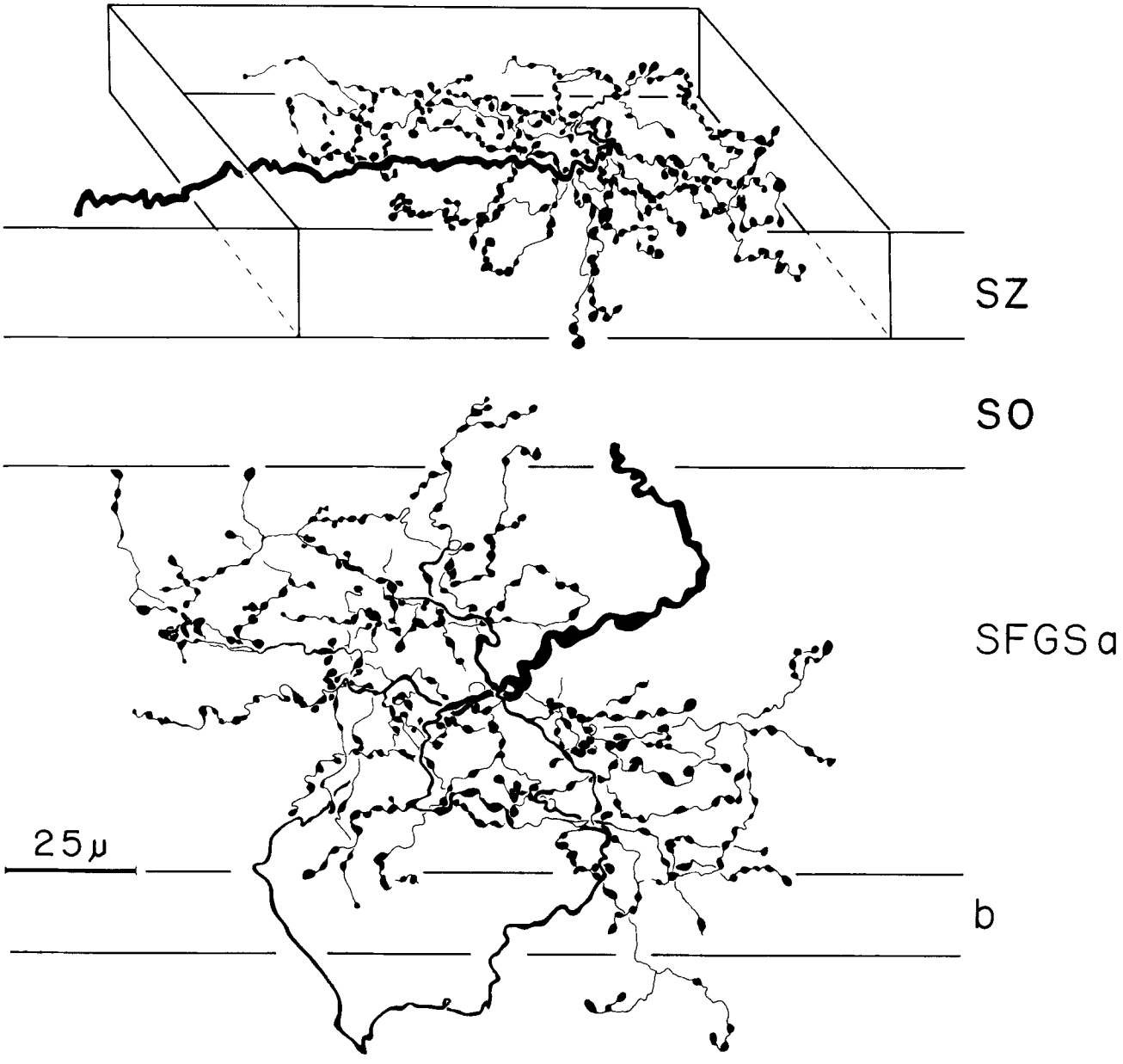

Fig. 11. Laminar variation in arbors with large-caliber axons. These arbors have axon diameters of about 2.0 μm and large boutons, also about 2.0 μm. The upper arbor was traced from an oblique section through the stratum zonale (indicated by the box surrounding it) and is about 100 μm along its long axis. The lower arbor is slightly larger, about 120 μm along its long axis.

increase in size with increasing size of their parent axon. This relationship is also evident in HRP-filled retinotectal arbors in two species of teleost fish (Ito et al., '84). Electron microscopic studies of retinal terminal boutons in cat superior colliculus show that they can be divided into subpopulations of small and large boutons (Behan, '81; Mize, '83) that may be derived from ganglion cell classes with small- and large-caliber axons, respectively (McIlwain and Lufkin, '76; McIlwain, '78; Itoh et al., '81). The significance, if any, of bouton size is not known. In snakes (Reperant et al., '81), as well as several teleost species (Airhart and Kriebel, '84; Ito et al., '80; Meek, '81), frogs (Lazar, '84), birds (Acheson et al., '80), and mammals (Lund, '69, '72; Behan, '81; Mize, '83), retinotectal boutons of all sizes show some similarities in vesicle size and shape, mitochondrial staining, and the morphology of the synaptic cleft. It has been noted in cat colliculus, however, that small boutons have a distinct, scalloped shape and make a larger number of synaptic contacts. Moreover, these contacts were more often involved in synaptic triads with vesicle-containing dendrites (Behan, '81; Mize, '83). Thus, size differences in boutons may be related to the nature of their synaptic interactions.

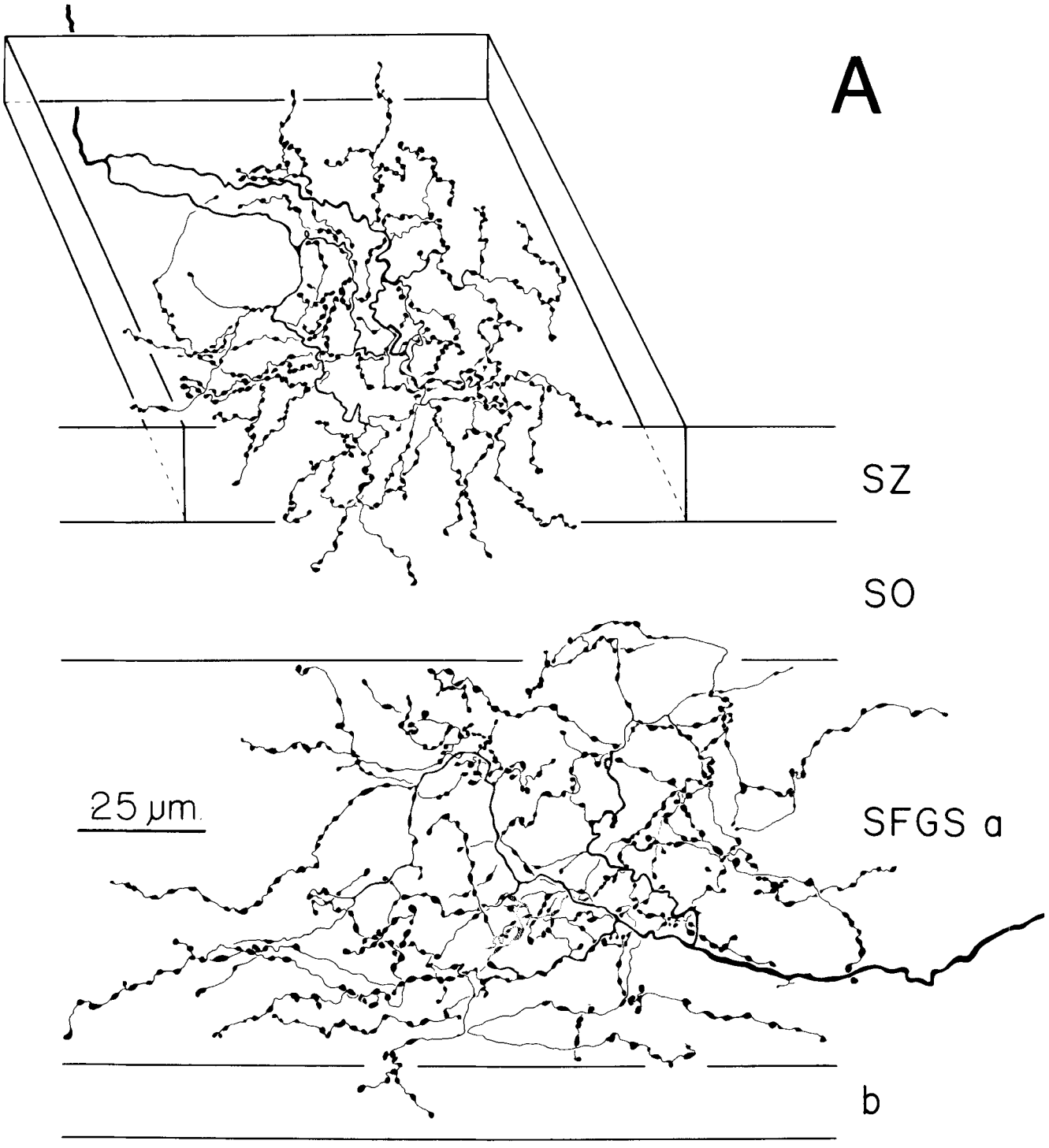

Fig. 12. Laminar variation in arbors with medium-caliber axons. This figure shows four arbors with axon diameters of about 1.0 μm. A. The upper arbor, in the stratum zonale, was traced from an oblique section (indicated by the box surrounding it) and its rostrocaudal extent is shown. This arbor measures about 90 μm in the mediolateral axis. The lower arbor in sublayer a of the stratum fibrosum et griseum superficiale is larger, about 125 μm in the mediolateral axis. B. Two arbors of about the same size (about 100 μm in the mediolateral axis) are shown in sublayers a and c of the stratum fibrosum et griseum superficiale. All of the arbors show a similar branching pattern and bear a great majority of medium-sized boutons that range from 1.0 to 1.5 μm along their long axes.

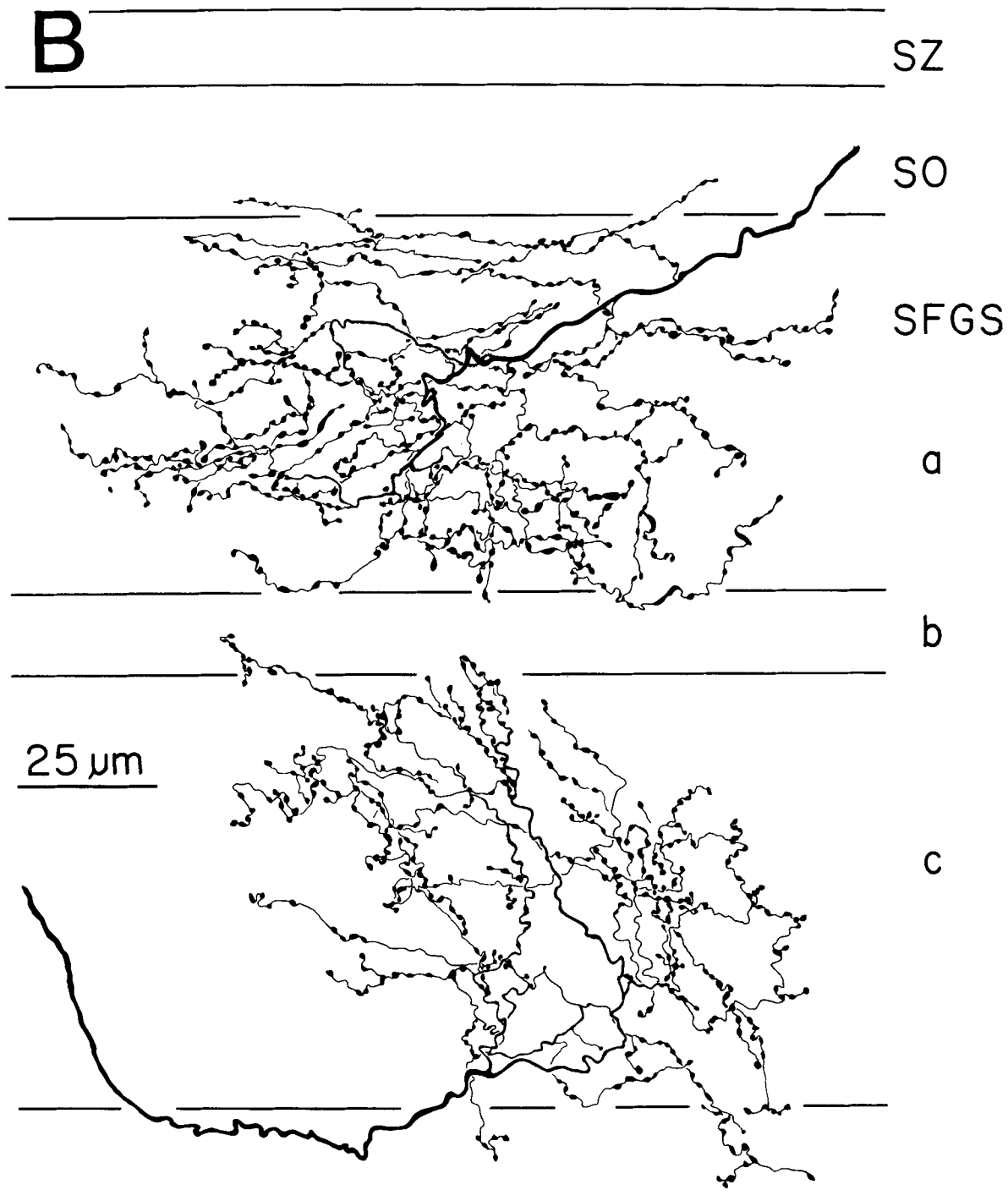

Figure 12 (cont'd)

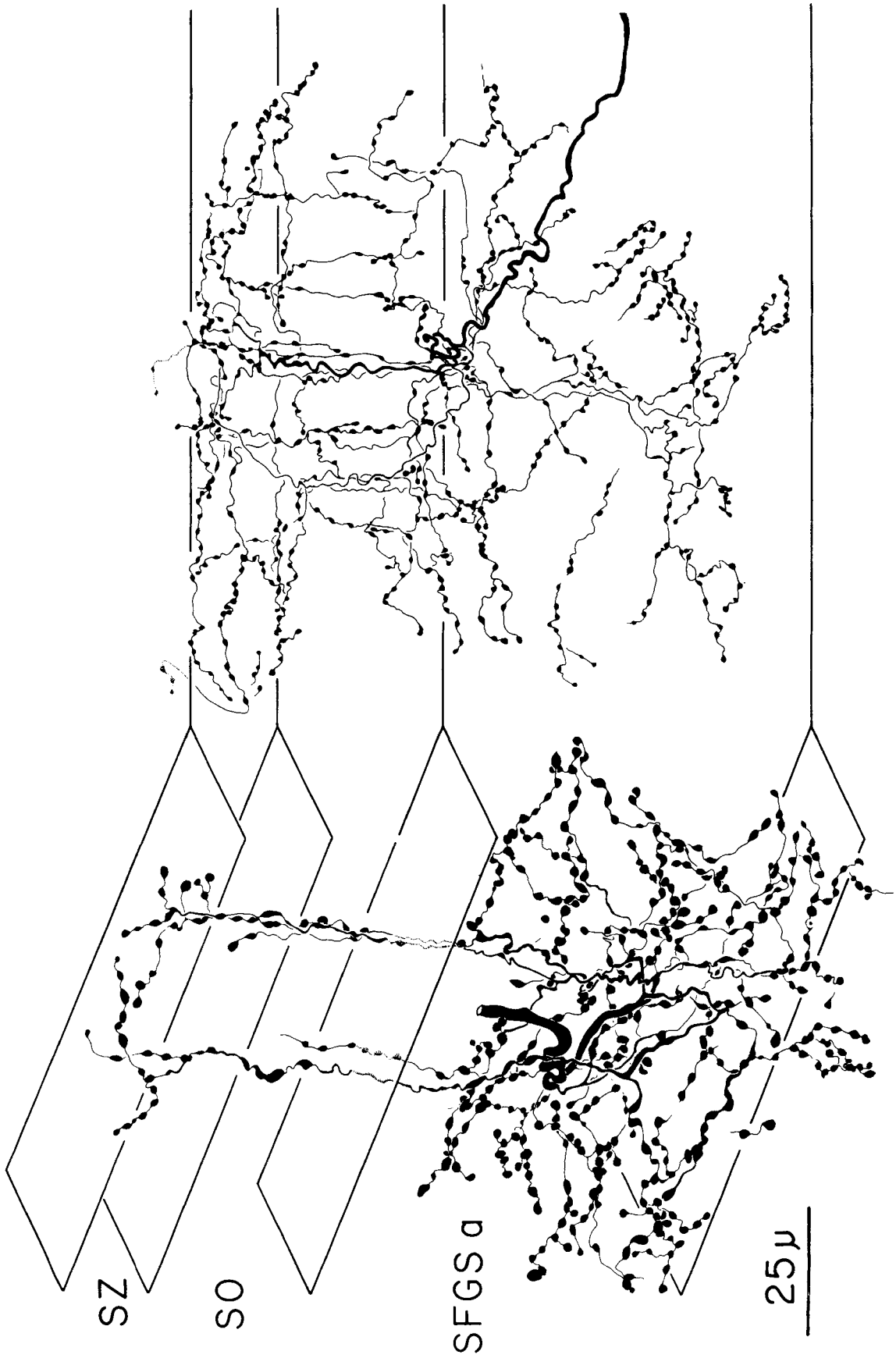

Fig. 13. Axons with arbors that extend across retinorecipient sublayers. Eight axons in the sample had branches that extended from sublayer a into the stratum opticum. The large-caliber axon on the left gives rise to terminal branchlets that extend through the stratum opticum into the stratum zonale. The medium-caliber axon on the right gives rise to terminal branchlets in sublayer a before it ascends through the stratum opticum and gives off preterminal branches and terminal branchlets in the stratum zonale.

Variation in the overall size of HRP-filled retinotectal arbors has also been observed in frogs (Potter, '72; Stirling and Merrill, '85) and hamsters (Sachs and Schneider, '84). In *Thamnophis* the size variation was not related to axon diameter; axons of all sizes gave rise to arbors that varied from 50 to 150 μm. Stirling and Merrill ('85), using intracellular injections of HRP, have recently shown that arbors derived from a single physiological class of ganglion cell in frogs may vary significantly in their overall size, and that this is related to differences in the receptive field structure among these ganglion cells. HRP fills of retinal arbors in hamster tectum suggest that variation in arbor size may be related to axon diameter and also to location in the tectal map (Sachs and Schneider, '84), though the systematic relation between arbor size and tectal magnification factor remains to be studied. Variation in arbor size is not related to either laminar position or to location in the tectum in *Thamnophis*.

In summary, studies of HRP-filled retinal terminal arbors in the tectum of a variety of vertebrates have demonstrated morphological variation in arbor size, branching patterns, parent axon diameter, and bouton size. How this complex variation is related to variation in ganglion cell morphology and the classification of ganglion cells into functional types remains to be determined.

Relation of retinal arbors to tectal neurons

The three retinorecipient sublayers defined by autoradiography correspond to regions occupied by the terminal arbors of single retinal axons. There is no apparent relation between the sublayer in which a terminal is located and its morphology. These results suggest that in *Thamnophis* retinotectal axons of different diameters do not show a laminar segregation and would predict that the distinct sublayers do not reflect segregation of narrow conduction velocity groupings or, by implication, single classes of retinal ganglion cells. A similar situation may be present in other species. In the lizard, *Dipsosaurus dorsalis* (Peterson, '81), both fine- and coarse-caliber fibers occur in each of three retinorecipient layers as assessed by silver degeneration. A range of bouton sizes from small to large occurs in each of three terminal sublayers in pigeons (Hunt and Webster, '75; Acheson et al., '80; Duff et al., '81). In monkeys (Marrocco, '78) and hamsters (Rhoades and Chalupa, '79), fast- and slow-conduction-velocity groups of retinocollicular axons do not show a laminar segregation.

By contrast, there is physiological evidence in other species for a laminar segregation of different conduction-velocity groups of retinotectal axons. In frogs a precise laminar segregation of classes of retinotectal inputs has been demonstrated with a variety of physiological and morphological techniques (Lettvin et al., '61; Maturana et al., '60; Chung et al., '74; George and Marks, '74; Stirling and Merrill, '85). A laminar organization of retinotectal inputs based on conduction velocity has also been reported in a salamander (Grusser-Cornehls and Himstedt, '73) and in two species of teleost fish (Vanegas et al., '71; Schmidt, '79). Some degree of laminar segregation has also been shown in slow- and fast-conducting axons to the cat and rat superior colliculus (McIlwain and Lufkin, '76; McIlwain, '78; Fukada et al., '78a).

These differences among species in the degree of laminar segregation of retinotectal axons may reflect differences in the relation of retinal afferents to tectal neurons. In frogs, tectal cells may receive inputs from specific classes of ganglion cells (review: Ewert, '84). In cats (Ogawa and Takahashi, '81; Berson and McIlwain, '82), rats (Fukada et al., '78b), and monkeys (Marrocco and Li, '77), tectal cells may be driven by specific conduction-velocity groupings of retinal inputs. The morphology of tectal neurons suggests that the three-tiered retinal terminal zone may serve to isolate a set of retinal inputs to specific classes of tectal efferent and intrinsic neurons in *Thamnophis* (Dacey and Ulinski, '86b,c). Of the efferent neurons, the tectoisthmi cells have a single, massive dendritic plexus that is confined to the stratum zonale. By contrast, tectoisthmobulbar cells have a similar plexus that fills sublayer a of the stratum fibrosum et griseum superficiale. Tectorotundal and tectogeniculate cells have dendrites that may extend across the entire extent of the retinorecipient zone, but arborize more heavily in sublayers a and c, respectively. Similarly, two classes of intrinsic neurons have dendritic arbors restricted to single sublayers. The type C cell has thin, appendage-laden dendrites that arborize in sublayer c, and the type B cell has thick, bulbous dendrites restricted to sublayer a of the stratum fibrosum et griseum superficiale. Consistent with this view, the morphology of many of the nonretinal afferents that project to the superficial tectal layers obeys the same laminar boundaries as the retinal arbors. These nonretinal afferents are the subjects of the next paper in this series (Dacey and Ulinski, '86d).

ACKNOWLEDGMENTS

This work was supported by PHS grant NS 12518. Shirley Aumiller and Maryellen Kurek provided assistance with photography. Vanessa Clemons typed the manuscript.

LITERATURE CITED

Acheson, D.W.K., S.K. Kemplay, and K.E. Webster (1980) Quantitative analysis of optic terminal profile distribution within the pigeon optic tectum. Neuroscience *5*:1067–1084.

Airhart, M.J., and R.M. Kriebel (1984) Retinal terminals in the goldfish optic tectum: Identification and characterization. J. Comp. Neurol. *226*:377–390.

Behan, M. (1981) Identification and distribution of retinocollicular terminals in the cat: An electron microscopic autoradiographic analysis. J. Comp. Neurol. *199*:1–15.

Berson, D.M., and J.T. McIlwain (1982) Retinal Y-cell activation of deep layer cells in superior colliculus of the cat. J. Neurophysiol. *47*:700–714.

Chung, S.H., T.V.P. Bliss, and M.J. Keating (1974) The synaptic organization of optic afferents in the amphibian tectum. Proc. R. Soc. Lond. [Biol.] *187*:421–447.

Colonnier, M. (1964) The tangential organization of the visual cortex. J. Anat. *98*:327–344.

Dacey D.M. (1984) Light microscopy of HRP-filled cat retinal ganglion cells. Neurosci. Abstr. *10*:838.

Dacey, D.M., and P.S. Ulinski (1986a) Optic tectum of the eastern garter snake, *Thamnophis sirtalis*. I. Efferent Pathways. J. Comp. Neurol. *245*:1–28.

Dacey, D.M., and P.S. Ulinski (1986b) Optic tectum of the eastern garter snake, *Thamnophis sirtalis*. II. Morphology of efferent cells. J. Comp. Neurol. *245*:198–237.

Dacey, D.M., and P.S. Ulinski (1986c) Optic tectum of the eastern garter snake, *Thamnophis sirtalis*. III. Morphology of intrinsic neurons. J. Comp. Neurol. *245*:283–300.

Dacey, D.M., and P.S. Ulinski (1986d) Optic tectum of the eastern garter snake *Thamnophis sirtalis*. V. Morphology of brainstem afferents and general discussion. J. Comp. Neurol. *245*:423–453.

Duff, T.A., G. Scott, and R. Mai (1981) Regional differences in pigeon optic tract, chiasm and retinoreceptive layers of optic tectum. J. Comp. Neurol. *198*:231–248.

Ewert, J. P. (1984) Tectal mechanisms that underlie prey-catching and avoidance behavior in toads. In H. Vanegas (ed): Comparative Neurology of the Optic Tectum. New York: Plenum Press, pp. 247–416.

Fukada, Y., D.A. Suziki, and K. Iwama (1978a) Characteristics of optic nerve innervation in the rat superior colliculus as revealed by field potential analysis. Jpn. J. Physiol. *29*:347–365.

Fukda, Y., D.A. Suziki, and K. Iwama (1978b) A four group classification of the rat superior collicular cells responding to optic nerve stimulation. Jpn. J. Physiol. *28*:367–384.

George, S.A., and W.B. Marks (1974) Optic nerve terminal arbors in the frog: Shape and orientation inferred from electrophysiological measurements. Exp. Neurol. *42*:467–482.

Geri, G.A., R.A. Kimsey, and C.A. Dvorak (1982) Quantitative electron microscopic analysis of the optic nerve of the turtle, *Pseudemys*. J. Comp. Neurol. *207*:99–103.

Grusser-Cornehls (1984) The neurophysiology of the amphibian optic tectum. In H. Vanegas (ed): Comparative Neurology of the Optic Tectum. New York: Plenum Press, pp. 211–246.

Grusser-Cornehls, U., and W. Himstedt (1973) Responses of retinal and tectal neurons of the salamander (*Salamandra salamandra L.*) to moving visual stimuli. Brain Behav. Evol. 7:145–168.

Halpern, M., and N. Frumin (1973) Retinal projections in a snake (*Thamnophis sirtalis*). J. Morphol. *141*:359–382.

Hunt, S.P., and K.E. Webster (1975) The projection of the retina upon the optic tectum in the pigeon. J. Comp. Neurol. *162*:433–446.

Ito, H., A.B., Butler, and S.O.E. Ebbesson (1980) An ultrastructural study of the normal synaptic organization of the optic tectum and the degenerating tectal afferents from retina, telencephalon and contralateral tectum in a teleoost, *Holocentrus rufus*. J. Comp. Neurol. *191*:639–660.

Ito, H., H. Vanegas, T. Murakami, and Y. Morita (1984) Diameters and terminal patterns of retinofugal axons in their target areas: An HRP study in two teleosts (*Sebastiscus* and *Navodon*). J. Comp. Neurol. *230*:179–197.

Itoh, I., M. Conley, and I.T. Diamond (1981) Different distributions of large and small retinal ganglion cells in the cat after HRP injections of single layers of the lateral geniculate body and the superior colliculus. Brain Res. *207*:147–152.

Kolb, H. (1982) The morphology of the bipolar cells, amacrine cells and ganglion cells in the retina of the turtle *Pseudemys scripta elegans*.. Philos. Trans. R. Soc. Lond. [Biol.] *298*:355–393.

Kolb, H., R. Nelson, and A. Mariani (1981) Amacrine cells, bipolar cells and ganglion cells of the cat retina: A Golgi study. Vision Res. *21*:1081–1114.

Lazar, G. (1984) Structure and connections of the frog optic tectum. In H. Vanegas (ed): Comparative Neurology of the Optic Tectum. New York: Plenum Press, pp. 185–210.

Lazar, G., and G. Szekely (1967) Golgi studies on the optic center of the frog. J. Hirnforsch. *9*:329–344.

Lettvin, J.Y., H.R. Maturana, W.H. Pitts, and W.S. McCulloch (1961) Two remarks on the visual system of the frog. In W.A. Rosenblith (ed): Sensory Communication. Cambridge: MIT Press, pp. 757–776.

Leventhal, A.G., R.W. Rodieck, and B. Dreher (1985) Central projections of cat retinal ganglion cells. J. Comp. Neurol. *237*:216–226.

Lund R.D. (1969) Synaptic patterns of the superficial layers of the superior colliculus of the rat. J. Comp. Neurol. *135*:179–208.

Lund R.D. (1972) Synaptic patterns in the superficial layers of the superior colliculus of the monkey, (*Macaca mulatta*) Exp. Brain Res. *15*:194–211.

Marchiafava, P.L., and R. Weiler (1980) Intracellular analysis and structural correlates of the organization of inputs to ganglion cells in the retina of the turtle. Proc. R. Soc. Lond. [Biol.] *208*:103–113.

Marchiafava, P.L., and H.G. Wagner (1981) Interaction leading to colour opponency in ganglion cells of the turtle retina. Proc. R. Soc. Lond. [Biol.] *211*:261–267.

Marrocco R.T. (1978) Conduction velocities of afferent input to superior colliculus in normal and decorticate monkeys. Brain Res. *140*:155–158.

Marrocco, R.T., and R.H. Li (1977) Monkey superior colliculus: Properties of single cells and their afferent inputs. J. Neurophysiol. *40*:844–860.

Maturana, H.R., J.Y. Lettvin, W.S. McCulloch, and W.H. Pitts (1960) Anatomy and physiology of vision in the frog (*Rana pipiens*). J. Gen. Physiol. *43*:129–175.

Meek, J.A. (1981) A Golgi-electron microscopic study of the goldfish optic tectum. I. Description of afferents, cell types, and synapses. J. Comp. Neurol. *199*:149–174.

McIlwain, J.T. (1978) Cat superior colliculus: Extracellular potentials related to W-cell synaptic actions. J. Neurophysiol. *41*:1343–1358.

McIlwain, J.T., and R.B. Lufkin (1976) Distribution of direct Y-cell inputs to the cat's superior colliculus: Are there spatial gradients? Brain Res. *103*:133–138.

Mize, R.R. (1983) Variations in the retinal synapses in the cat superior colliculus revealed using quantitative electron microscope autoradiography Brain Res. *269*:211–221.

Ogawa, T., and Y. Takahashi (1981) Retinotectal connectivities within the superficial layers of the cat's superior colliculus. Brain Res. *217*:1–11.

Peterson, E.H. (1981) Regional specialization in the retinal ganglion cell projection to optic tectum of *Dipsosaurus dorsalis (Iguanidae)*. J Comp. Neurol. *196*:225–252.

Peterson, E.H., and P.S. Ulinski (1982) Quantitative studies of retinal ganglion cells in a turtle *Pseudemys scripta elegans*. II. Size spectrum of ganglion cells and its regional variation. J. Comp. Neurol. *208*:157–168.

Potter, H.D. (1972) Terminal arborizations of retinotectal axons in the bullfrog. J. Comp. Neurol. *144*:269–284.

Quiroga, J.C. (1978) The tectum opticum of *Pantodactylus schreiberri* (Teiidae Lacertillia, Reptilia). J. Hirnforsch. *19*:109–131.

Ramón y Cajal, S. (1911) Histologie du Systeme Nerveux de l'Homme et des Vertebres. Vol. 2, Consejo Superior de Investigaciones Cientificas, Instituto Ramon y Cajal, Madrid (1954) pp. 174–226.

Ramón y Cajal, S. (1933) La retine des vertebres. Trab. Lab. Invest. Biol Univ. Madrid *28*:1–141.

Reperant, J., J. Peyrichoux, and J.P. Rio (1981) Fine structure of the superficial layers of the viper optic tectum. A Golgi and electron microscopic study. J. Comp.. Neurol. *199*:393–417.

Rhoades, R.W., and L.M. Chalupa (1979) Conduction velocity distribution of the retinal input to the hamster's superior colliculus and a correlation with receptive field characteristics. J.Comp. Neurol. *184*:243–264.

Rodieck R.W. (1979) Visual pathways. Ann. Rev. Neurosci.*2*:193–226.

Sachs, G.M., and G.E. Schneider (1984) The morphology of optic tract axons arborizing in the superior colliculus of the hamster. J. Comp. Neurol. *230*:155–167.

Schmidt, J.T. (1979) The laminar organization of optic nerve fibers in the optic tectum of goldfish. Proc. R. Soc. Lond. [Biol.] *205*:287–306.

Stone, J., and J.A. Freeman (1971) Synaptic organization of the pigeon optic tectum: A golgi and current source-density analysis. Brain Res. *27*:203–221.

Stirling, R.V, and E.G. Merrill (1985) Quantitative relationships between morphology and receptive field characteristics of frog "off" centre ganglion cells stained with horseradish peroxidase (HRP). Neurosci. Abstr. *11*:237.

Valverde, F. (1970) The Golgi method. A tool for comparative structural analyses. In W.J.H. Nauta and S.O.E. Ebbesson (eds): Contemporary Research Methods in Neuroanatomy. New York: Springer Verlag, pp 12–31.

Vanegas, H., E. Essayag-Millan, and M. Laufer (1971) Response of optic tectum to stimulation of the optic nerve in the teleost *Eugerres plumieri*. Brain Res. *73*:151–155.

Vanegas, H., B. Williams, and E. Essayag (1984) Electrophysiological and behavioral aspects of the teleostean optic tectum. In H. Vanegas (ed): Comparative Neurology of the Optic Tectum. New York: Plenum Press, pp. 121–162.